



Effect of Initial Grain Size on the Dynamic Recrystallization of Hot Deformation for 3003 Aluminum Alloy

Guiqing Chen¹ · Gaosheng Fu² · Tianyun Wei¹ · Chaozeng Cheng² · Huosheng Wang³ · Junde Wang⁴

Received: 18 October 2017 / Accepted: 26 December 2017 / Published online: 16 March 2018
© The Korean Institute of Metals and Materials 2018

Abstract

The 3003 aluminum alloys with four different initial grain sizes were deformed by isothermal compression in the range of deformation temperature 300–500 °C at strain rate 0.01–10.0 s⁻¹ with Gleeble-1500 thermal simulator. The results show that the smaller the initial grain size of the alloy, the greater the required deformation resistance, and the smaller the peak strain, which is conducive to the occurrence of dynamic recrystallization (DRX). The DRX critical strain increases with the decrease of the deformation temperature or the increase of the strain rate, and the DRX volume fraction increases with the decrease of the strain rate and the increase of the deformation temperature. The average grain size of 3003 aluminum alloy after deformation is smaller than that before deformation. The smaller the initial grain size, the lower the critical recrystallization strain. So the DRX is carried out more fully, contributing to the thermoplastic deformation of the alloy.

Keywords 3003 Aluminum alloy · Initial grain size · Critical strain · DRX volume fraction

1 Introduction

The internal structure of the alloy usually undergoes three change stages during the high temperature plastic deformation, namely, work hardening, dynamic recovery and DRX. DRX is an extremely important microstructure evolution in the process of hot deformation [1–3]. It plays an important role in the microstructure changes of 3003 aluminum alloy during hot deformation, which not only can reduce the dislocation propagation and plugging effect caused by the work hardening to achieve the effect of dynamic softening, but also can refine the grain, thereby enhancing the plasticity and toughness of the alloy. Therefore, DRX softening behavior of the alloy during the hot deformation has become the focus of attention. DRX process of the alloy is closely

related to its chemical composition, the original microstructure state and hot deformation conditions. DRX occurs only at a certain deformation temperature, strain rate and deformation [4]. Therefore, it is necessary to quantitatively study the evolution law of DRX structure, which not only can provide the correct prediction model for the numerical simulation of microstructure and performance, but also can provide experimental basis for optimizing the hot deformation process parameters of 3003 aluminum alloy and formulating “precise control” scheme. The dynamic softening behavior of the 3003 aluminum alloy is affected by the initial grain size of the alloy in addition to the hot deformation conditions [5–7]. It is necessary to combine the two factors in order to further reveal the influence of the initial grain size on the dynamic softening behavior of 3003 aluminum alloy.

✉ Gaosheng Fu
fugaosheng@fzu.edu.cn

¹ Department of Mechanical Engineering, Fujian Chuanzheng Communications College, Fuzhou 350007, China

² College of Materials Science and Engineering, Fuzhou University, Fuzhou 350108, China

³ College of Materials Science and Engineering, Fujian University of Technology, Fuzhou 350118, China

⁴ Department of Mechanical Engineering, Changji Vocational and Technical College, Changji 831100, China

2 Experimental Procedure

The main components of the 3003 aluminum alloy are (mass fraction/%): 0.62 Fe, 0.58 Si, 1.09 Mn, 0.068 Cu, 0.006 Ti, 0.03 Mg, 0.007 Ni, 0.008 Zn, the balance being Al. The preparation of the ingot is: firstly, the aluminum ingots were subjected to four different melt treatments in a graphite crucible resistance furnace [8], that is, untreated (UT), conventional purification (CPT), efficient purification

(EPT) and efficient integrated treatment (EIT). Secondly, pour out the ingot, heat treatment (510 °C, 20 h). Finally, process the hot compression samples according to the standard. Cylindrical specimens of 10 mm in diameter and 15 mm in height were machined for hot compression tests. The both flat ends of the specimen were recessed to a depth of 0.2 mm deep around to entrap graphite powder in order to minimize the friction between the specimen surface and clamp. The samples were mounted on a Gleeble-1500 thermal simulator for isothermal constant strain rate hot compression test. The experimental conditions for the hot deformation are: the heating rate of the sample is controlled at 1 °C/s, insulation for 5 min after the set temperature. Control the amount of compression deformation of 0.7. The range of strain rate is 0.01–10.0 s⁻¹, and the deformation temperature is in the range of 300–500 °C. The data of the experiment is controlled and collected by the computer. The deformed specimens were quenched in water quickly after each compression test in order to maintain the microstructure.

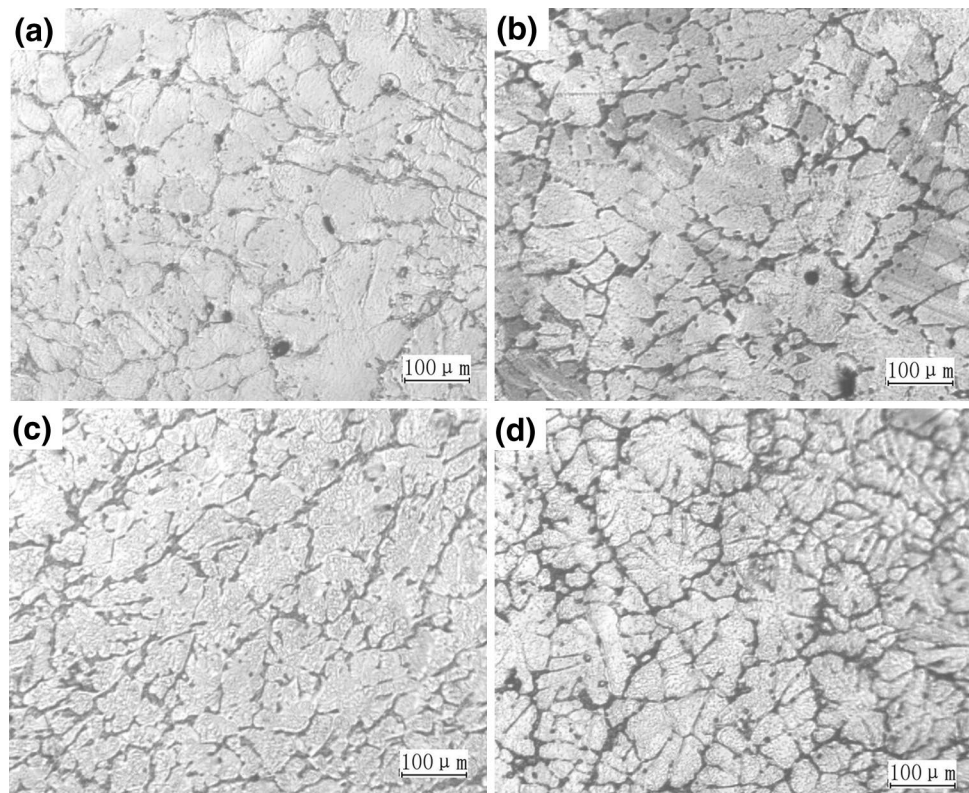
For microstructural examination, the specimens were sliced parallel to the direction of compression. The microstructure characterization of the deformed samples were observed by using XJG-05 optical microscope (OM), ZEISS EVO MA10 electron backscatter diffraction (EBSD) and

JEM-2100F transmission electron microscopy (TEM). To take microscopic examination, the specimens were mechanical polished and etched with Keller's reagent (2.5 ml HNO₃, 1.5 ml HCl, 1 ml HF and 95 ml H₂O). The foils used for TEM were prepared by mechanical polishing to less than 80 μm and then punched into 5 mm discs. Finally, twin-jet electro-polishing device was carried out on preparation of the sample with an electrolyte solution of 25% nitric acid and 75% methanol at the voltage of ~ 15 V DC and the temperature below -20 °C. It is remarkable to note that the samples used for EBSD were sprayed approximately 45 s while the TEM samples were sprayed continually until appear a small hole. Figure 1 shows the heat-treated microstructures of 3003 aluminum alloys with four different melt treatments. For determination of grain sizes of annealed samples, average linear grain intercept lengths technique was used. Table 1 is the average grain size measured using an image analysis system.

Table 1 Average grain size of 3003 aluminum alloy

Melt treatment process	UT	CPT	EPT	EIT
Average grain size (μm)	94	79	68	51

Fig. 1 OM images of 3003 aluminum alloys with different melt treatments. **a** UT, **b** CPT, **c** EPT, **d** EIT



3 Results and Analysis

3.1 True Stress–Strain Curve

The true stress–true strain curves of 3003 aluminum alloys with four different grain sizes are shown in Figs. 2 and 3, which were deformed in the range of deformation temperature 300–500 °C at strain rate 0.01–10.0 s⁻¹.

As can be seen from Figs. 2 and 3, at the same strain rate, the flow stress decreases generally with the increase of the deformation temperature. Under the same deformation temperature conditions, the flow stress increases with the increase of the strain rate, indicating that the alloy is a positive strain rate sensitive material. At high strain rate (≥ 10.0 s⁻¹), the flow stress curve appears sawtooth fluctuation and the alloy undergoes discontinuous DRX. This is because the deformation time is short at high strain rate, the dynamic response produced by the slip of the screw dislocation and the movement of the edge dislocation is limited. Sub-grain boundary is not well formed, and the dislocation density within the grain is still kept at a high level, so that the internal storage energy of the metal can

be increased rapidly, to achieve the driving force required for DRX, and eventually lead to the occurrence of DRX [9, 10]. The peak flow stress of the same alloy under the same hot deformation condition is different. This is mainly related to the initial grain size of the alloy (Table 1) before the deformation. Such as at medium strain rate, the flow stress of the 3003 aluminum alloy with EIT is larger than that of 3003 aluminum alloy with UT. This is because the grain boundary plays a hindrance on the dislocation slip. The 3003 aluminum alloy with EIT has the smaller grain size and the more grain boundary, so the more stress is required for the dislocation slip. But with the deformation temperature rising, the flow stress of 3003 aluminum alloy with EIT is slightly smaller than that of 3003 aluminum alloy with UT. When the deformation temperature is high, due to the increase of atomic activity, as well as the diffusion rate of atoms along the grain boundary accelerates, so that the grain boundary at high temperatures has a certain viscosity characteristics. Its resistance to deformation is greatly weakened, even if the application of a small stress, as long as the action time is long enough, there will be grain along the grain boundary relative sliding. When the grain size is reduced, the grain boundary area per unit

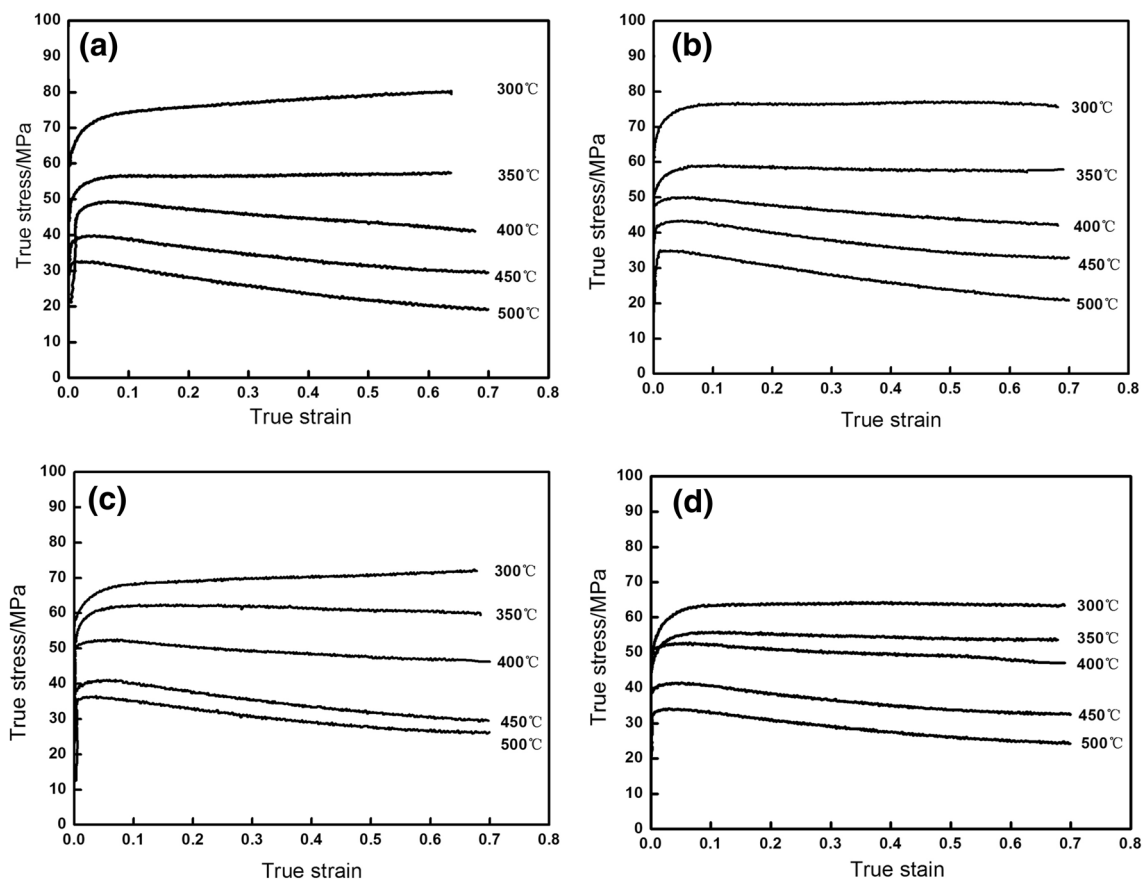


Fig. 2 True stress–true strain curves of 3003 aluminum alloy at the strain rate of 0.1 s⁻¹. **a** UT, **b** CPT, **c** EPT, **d** EIT

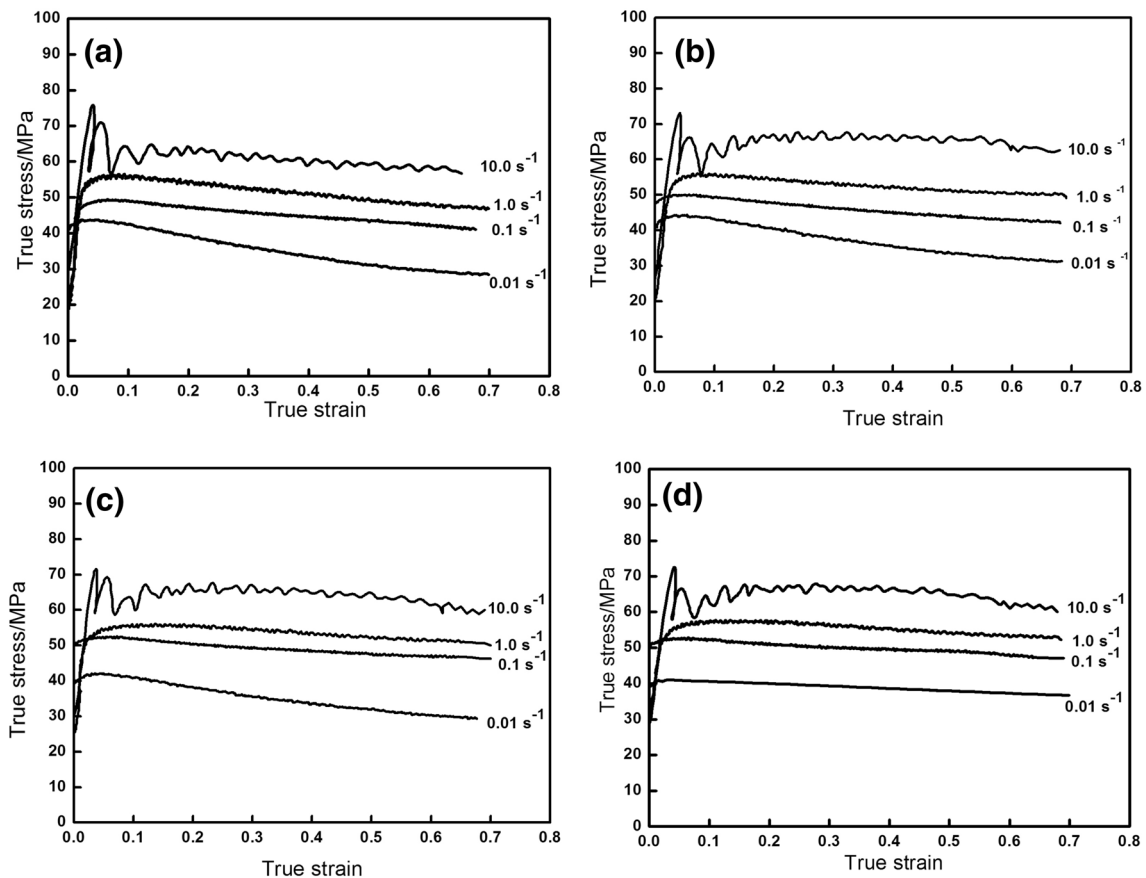


Fig. 3 True stress–true strain curves of 3003 aluminum alloy at the deformation temperature of 400 °C. **a** UT, **b** CPT, **c** EPT, **d** EIT

volume increases, and the grain boundary viscosity is strengthened, thus reducing the flow stress [11].

3.2 Comparison of DRX Critical Strain

When the deformation temperature and strain rate are constant, the change rate of stress changing with the strain is called the strain hardening rate [12]:

$$\theta = \left(\frac{d\sigma}{d\varepsilon} \right)_{\varepsilon, T} \quad (1)$$

The relationship between the strain hardening rate and the flow stress can better reveal the microstructure changes during the hot deformation, and can more accurately determine the characteristic value of the flow stress curve. E. I. Poliak and J. J. Jonas proposed a dynamical critical condition based on the thermodynamic irreversible principle. It is assumed that the critical condition corresponds to the minimum value on the $(-\partial\theta/\partial\sigma) \sim \sigma$ curve or the inflection point on the $\ln \theta \sim \varepsilon$ curve. The strain value corresponding to the inflection point or the minimum value is the critical strain (ε_c) of the DRX, and the corresponding stress is the critical stress (σ_c). According to the Eq. (1), the relationship

curves of 3003 aluminum alloy with UT between $\theta \sim \sigma$ and $(-\partial\theta/\partial\sigma) \sim \sigma$ can be determined, as shown in Fig. 4.

The flow stress corresponding to $\frac{\partial}{\partial\sigma} \left(-\frac{\partial\theta}{\partial\sigma} \right) = 0$ is the DRX critical stress (σ_c). It can be obtained directly from the $(\partial\theta/\partial\sigma) \sim \sigma$ curve, and the critical strain (ε_c) can be obtained from the DRX critical stress of the flow stress curve, the calculation results are shown in Table 2.

It can be seen from Table 2 that the DRX critical strain value of 3003 aluminum alloy increases with the increase of Z (Zener-Hollomon) parameter (decrease of deformation temperature or increase of strain rate), this is because the deformation temperature is reduced, the climb and slip of the dislocation are hindered, and sub-grain formation and merger are difficult, which make the DRX difficult occur in the hot deformation process, resulting in increased DRX critical strain value. On the other hand, the process of DRX is closely related to time. The deformation time is shortened with the increase of the strain rate, and the movement and climbing of the dislocations are difficult to be carried out. It affects the DRX nucleation quantity, limits the growth rate of the recrystallized grains, and weakens the softening effect of the DRX, which lead to the increase of the critical strain value obtained by the balance of

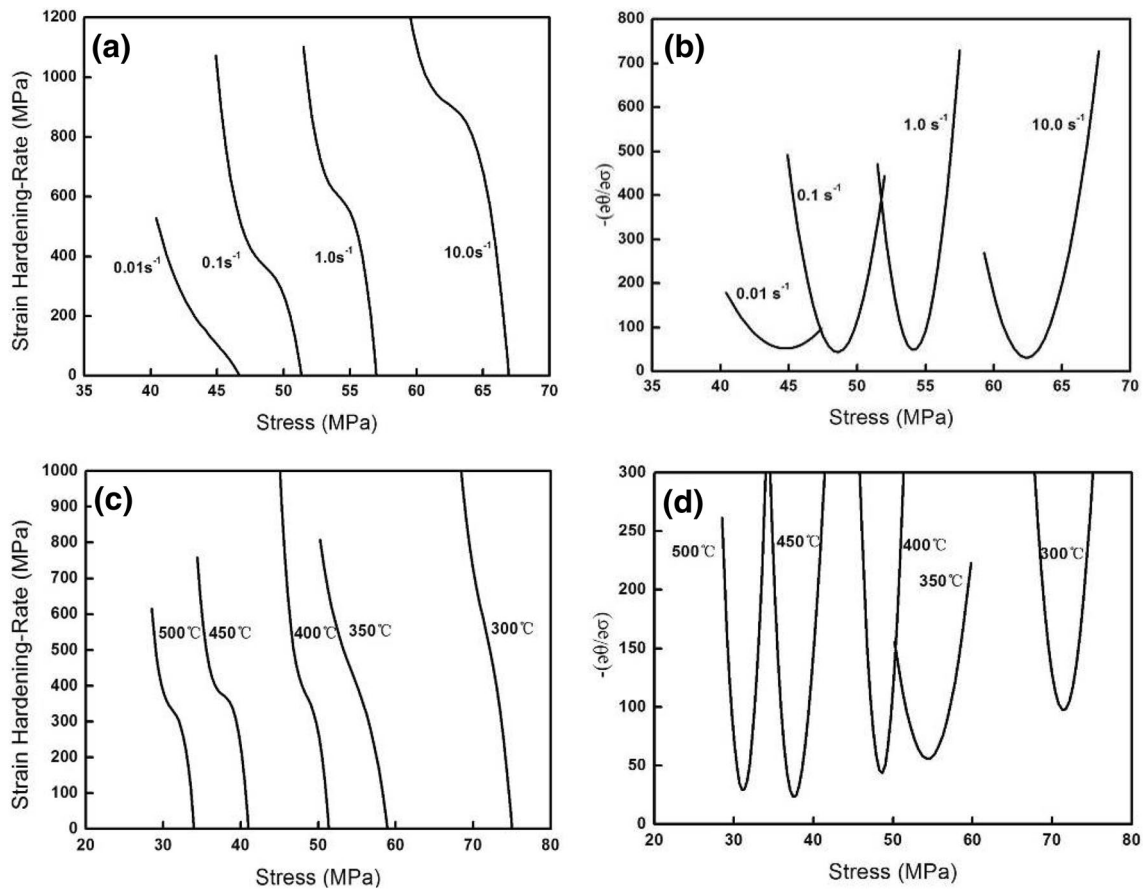


Fig. 4 Curves between strain hardening rate and flow stress under different deformation conditions. **a** 400 °C, $\theta \sim \sigma$, **b** 400 °C, $(-\partial\theta/\partial\sigma) \sim \sigma$, **c** 0.1 s⁻¹, $\theta \sim \sigma$, **d** 0.1 s⁻¹, $(-\partial\theta/\partial\sigma) \sim \sigma$

Table 2 Critical strain values of 3003 aluminum alloys under different hot deformation conditions

Temperature (°C)	Strain rate (s ⁻¹)	UT	CPT	EPT	EIT
300	0.1	0.07916	0.07430	0.06597	0.06390
	0.01	0.05785	0.05797	0.05302	0.04789
	0.1	0.04477	0.04081	0.03732	0.03232
	1.0	0.03362	0.03615	0.03325	0.02563
	10.0	0.02571	0.02924	0.02172	0.01919
350	0.1	0.03065	0.03197	0.02922	0.02190
	0.01	0.04477	0.04081	0.03732	0.03232
	1.0	0.05368	0.05082	0.05021	0.04050
	10.0	0.07358	0.06687	0.05940	0.05624

strain hardening and DRX softening. At the same time, under the higher strain rate condition, the “adiabatic temperature rise effect” will be produced, which will increase the local temperature of the material and enhance the dynamic recovery effect. The dislocation will be canceled each other through the slip and climb, and the dislocation density will decrease.

Therefore, the internal residual deformation storage energy of the material can be reduced, and the DRX is difficult to occur, resulting in an increase in the DRX critical strain.

Under the same hot deformation conditions, the critical strain value of 3003 aluminum alloy with UT is the largest, followed by that of 3003 aluminum alloy with CPT and EPT, and the critical strain value of 3003 aluminum alloy with EIT is the smallest. Since the DRX is a hot activation process, the hot deformation activation energy of 3003 aluminum alloy with EIT is the lowest. When the local deformation occurs, it will start more slip system, and the metal absorbs more deformation energy, so as to achieve the driving force required for DRX. At the same time, the formation of high-density dislocation area increases the nucleation rate of the DRX, which reduces the critical strain of the DRX, leading to the occurrence of DRX.

3.3 Effect of Initial Grain Size on DRX Volume Fraction

To establish a DRX kinematic model, the DRX volume fraction must be measured firstly. According to the traditional

measurement of metallographic method, the result will inevitably be subject to metallographic corrosion and field selection. In this study, the DRX volume fraction is calculated from the eigenvalues of flow stress curve during the hot deformation [13, 14].

$$X_d = \frac{\sigma_{REC} - \sigma_{DRX}}{\sigma_{REC} - \sigma_s} \quad (2)$$

where X_d is the DRX volume fraction, σ_{REC} is the stress value on the flow stress curve when the metal does not undergo dynamic softening, σ_{DRX} is the stress value on the high temperature flow stress curve, and σ_s is the steady-state stress value of the high temperature flow stress curve. The meaning of the symbols in the Eq. (2) is shown in Fig. 5. According to the experimental data of thermodynamics, the actual flow stress and the DRX steady-state flow stress can be obtained. The dynamic recovery curve of the alloy can be obtained by nonlinear least squares fitting and extrapolation based on the flow stress curve data before DRX. The fitting mathematical model is [14]:

$$\frac{\sigma - \sigma_{0.2}}{\sigma_{ss} - \sigma_{0.2}} = (1 - e^{-c\epsilon})^M \quad (3)$$

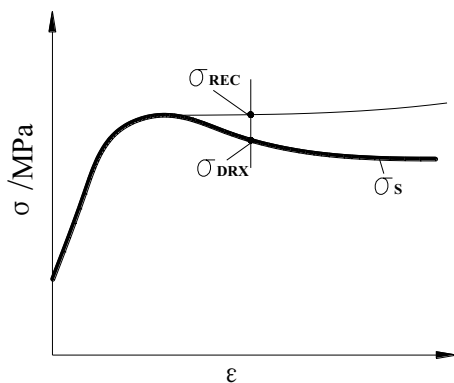


Fig. 5 Illustration of DRX volume fraction of metallic materials

where σ_{ss} is the steady-state stress value on the dynamic recovery flow stress curve, and C and M are constant coefficients.

According to Eqs. (2) and (3) and the experimental data of Fig. 1, the DRX volume fraction under different deformation conditions can be calculated, and the relationship curves of 3003 aluminum alloy with EIT between the DRX volume fraction and the deformation amount were plotted (Fig. 6). It can be seen that in the same deformation amount, the DRX volume fraction increases with the increase of deformation temperature or the decrease of the strain rate. This is because Z value decreased with the increase of deformation temperature, then the critical strain value of the DRX decreases, resulting in the DRX more likely to occur. In addition, the grain boundary migration ability is enhanced with the increasing deformation temperature, so that the nucleation rate of recrystallization increased, and DRX carried out more fully, that is, the high temperature or low strain rate is more favorable for the occurrence of DRX.

At the strain of 0.7, the DRX volume fraction of 3003 aluminum alloys with different grain sizes can be obtained by the same method, as shown in Table 3. The DRX volume fraction of 3003 aluminum alloys with different grain sizes under the same hot deformation condition are different.

The DRX volume fraction of 3003 aluminum alloy with UT is the smallest under given experimental conditions. From the previous analysis, it can be seen that the DRX critical strain of 3003 aluminum alloy with UT is the largest, and it is difficult to enter the steady-state deformation stage, so the DRX volume fraction is the lowest. Because the removal impurities efficiency of 3003 aluminum alloy

Table 3 DRX volume fraction (%) at the strain of 0.7 (400 °C, 0.1 s⁻¹)

Melt treatment	UT	CPT	EPT	EIT
DRX volume fraction	63.58	68.75	75.58	88.64

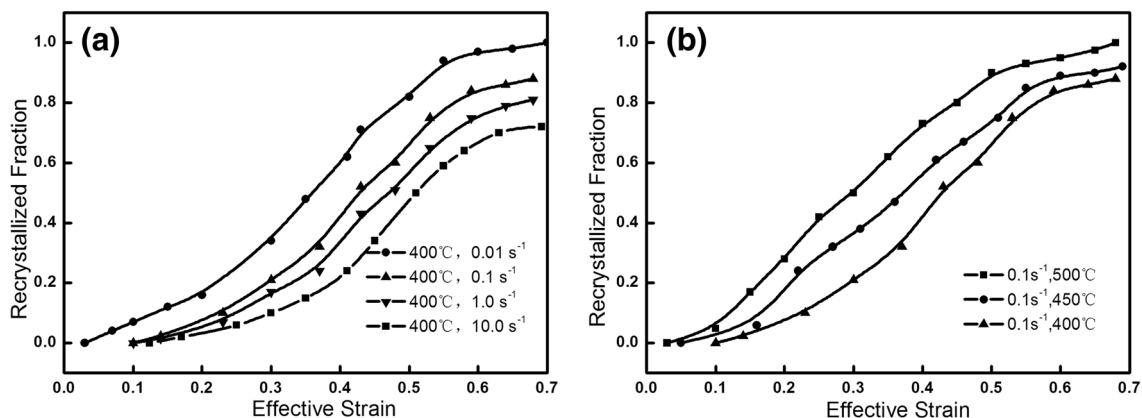


Fig. 6 DRX volume fraction curves under different deformation conditions. a 400 °C; b 0.1 s⁻¹

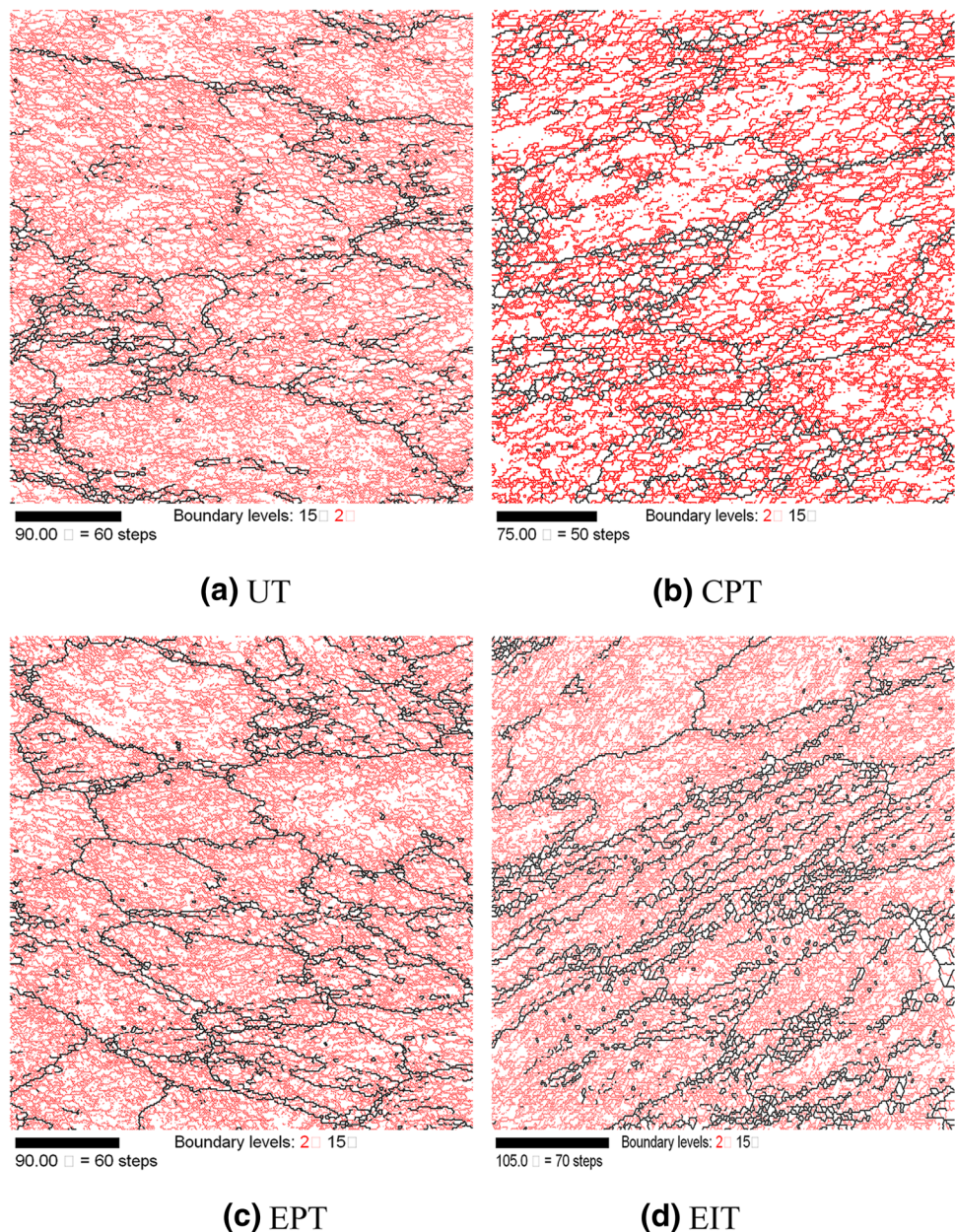
with CPT is not obvious and the hot deformation activation energy is large [7], the DRX is difficult to occur. Therefore, the DRX volume fraction of 3003 aluminum alloy with CPT is similar with that of 3003 aluminum alloy with UT. The DRX volume fraction of 3003 aluminum alloy with EPT has a certain degree of improvement, but the difference is not obvious. The initial grain size and distribution of the 3003 aluminum alloy with EIT is fine and uniform, whose internal metallurgical quality has been significantly improved, which is favorable for the thermoplastic deformation, so the DRX volume fraction of the alloy with EIT is the largest.

3.4 Effect of Initial Grain Size on Microstructure

The microstructure of the 3003 aluminum alloys with four different grain sizes at deformation temperature of 400 °C and strain rate of 0.1 s⁻¹ are shown in Fig. 7, and Fig. 8 shows the distribution of grain size.

It can be seen from Figs. 7 and 8 that under the same hot deformation condition, the 3003 aluminum alloy with UT has large grain size and uneven deformation structure, and the deformed grains are elongated. There are high dislocation densities in the grain boundaries. The dislocations intertwine with each other to form dislocation walls (Fig. 9a),

Fig. 7 EBSD images of 3003 aluminum alloy deformed at 400 °C, 0.1 s⁻¹. **a** UT **b** CPT **c** EPT **d** EIT



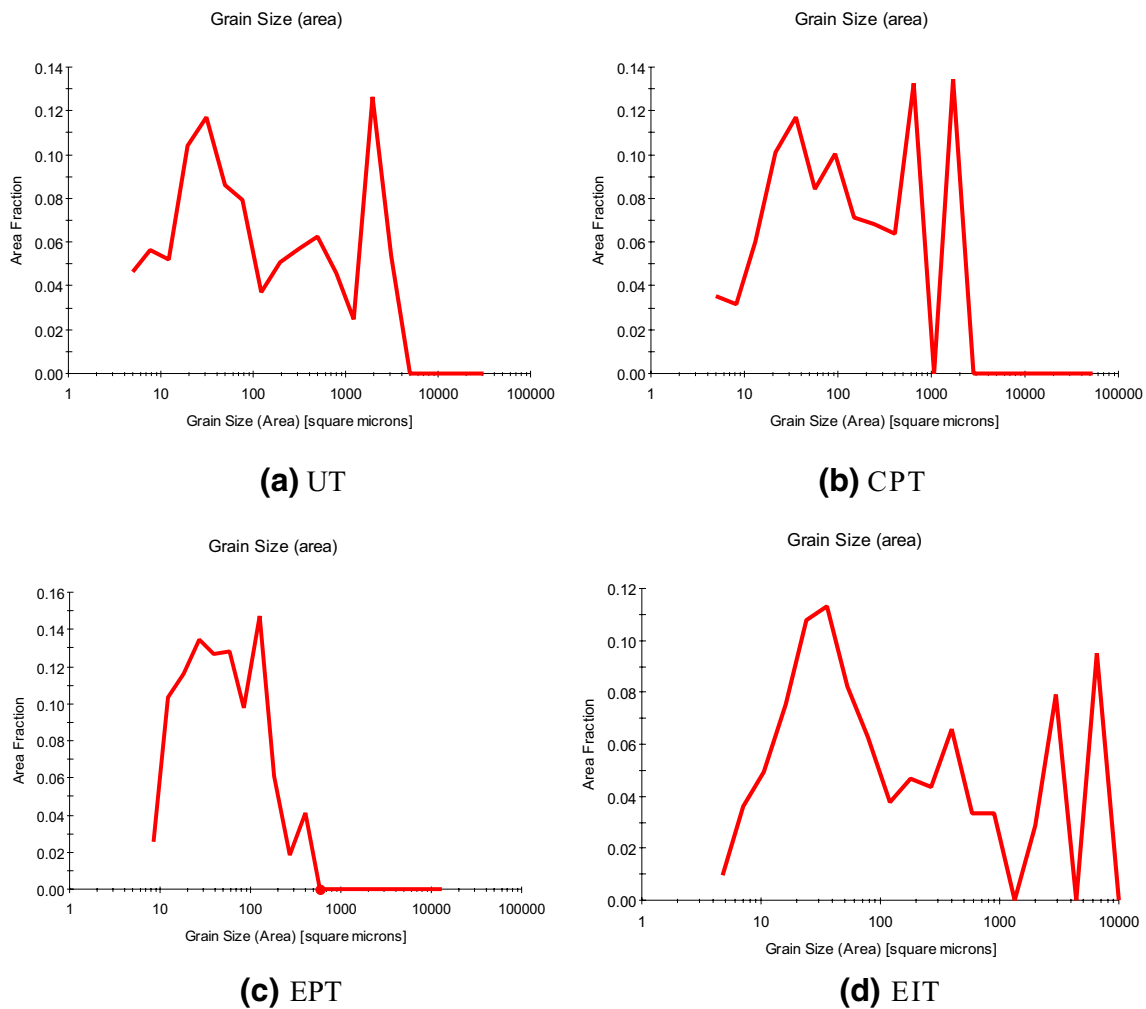


Fig. 8 Grain size distribution of 3003 aluminum alloy deformed at 400 °C, 0.1 s⁻¹. **a** UT **b** CPT **c** EPT **d** EIT

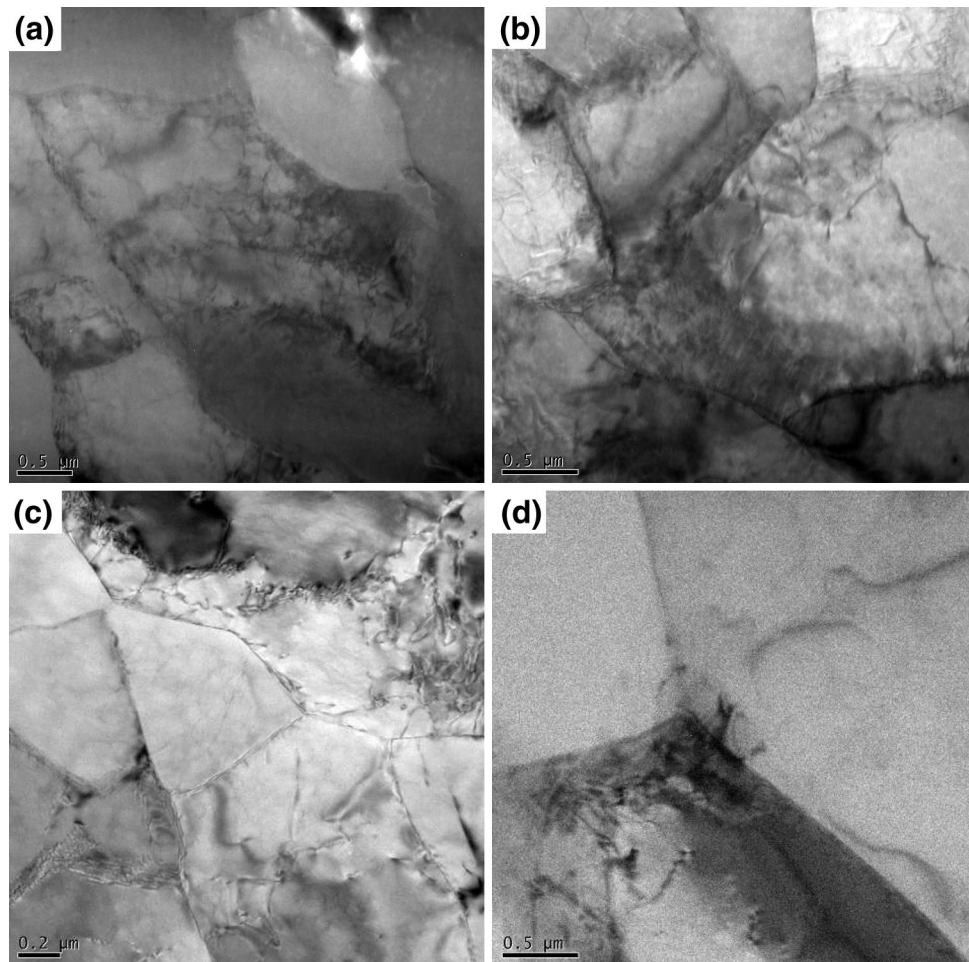
which has typical dynamic recovery characteristics. The grain sizes of 3003 aluminum alloy with CPT and EPT have been reduced, but still elongated. The density of dislocations in the alloy decreases and the sub-grains are merging (Fig. 9b). However, high-density dislocation networks still exist in the local area and partial DRX has begun to occur. The grain size of the 3003 aluminum alloy with EIT is further reduced, the grain is refined, and the grain boundary area increased. After the high temperature deformation, no obvious elongated grains were observed, which is essentially equiaxed. This is because the initial grain size (Table 1) of 3003 aluminum alloy with EIT is smallest and grain boundary area is also the largest. The grain boundary has good plasticity at high temperature, which can be carried out viscous flow. At the same time, small equiaxed grains can reduce the grain rotation and grain boundary sliding resistance, which is conducive to the thermoplastic deformation of the alloy. Dislocations disappear within the grain (Fig. 9d). The large-angle grains can be observed, and DRX carried

out more fully. Therefore, the observation of the microstructure is consistent with the result of Table 3, that is, smaller initial grain size is conducive to the occurrence of DRX.

4 Conclusions

1. The flow stress of 3003 aluminum alloys with different initial grain sizes increase with the increase of strain rate or the decrease of deformation temperature during hot deformation, indicating that the alloy is a positive strain rate sensitive material. The smaller the initial grain size, the greater the required deformation resistance, the smaller the peak strain, and the more prone to DRX.
2. The DRX critical strain increases with the decrease of deformation temperature or the increase of strain rate, and the DRX critical strain decreases with the decrease of initial grain size.

Fig. 9 The TEM images of 3003 aluminum alloy deformed at 400 °C, 0.1 s⁻¹. **a** UT, **b** CPT, **c** EPT, **d** EIT



- The DRX volume fraction increases with the decrease of strain rate or the increase of deformation temperature. The smaller the initial grain, the more complete the DRX.
- The average grain sizes of 3003 aluminum alloys with different initial grain sizes are smaller than that before deformation, and the fine uniform initial grain size is favorable for the thermoplastic deformation of the alloy.

Acknowledgements The authors would like to acknowledge the financial support from Fujian Natural Science Foundation (2017J01156, 2017J01083), Xinjiang Uygur Autonomous Region university scientific research program scientific research key project (XJEDU2016I068), Science and Technology Project of Fujian Education Department (JA15659), and materials nearly net forming and digital manufacturing technology service team of Fujian Chuazheng Communications College of China.

References

- T. Sakai, A. Belyakov, R. Kaibyshev, H. Miura, J.J. Jonas, *Prog. Mater. Sci.* **60**, 130 (2014)
- X.M. Chen, Y.C. Lin, D.X. Wen, J.L. Zhang, M. He, *Mater. Des.* **57**, 568 (2014)
- G. Chen, G. Fu, H. Chen, C. Cheng, W. Yan, S. Lin, *Met. Mater. Int.* **18**(5), 813 (2012)
- G. Chen, G. Fu, W. Yan, C. Cheng, Z. Zou, *Met. Sci. Heat Treat.* **55**(3–4), 220 (2013)
- H.R. Rezaei Ashtiani, M.H. Parsa, H. Bisadi, *Mater. Des.* **42**, 478 (2012)
- R. Fan, J. Magargee, P. Hu, J. Cao, *Mater. Sci. Eng. A* **574**, 218 (2013)
- G. Chen, G. Fu, H. Chen, W. Yan, C. Cheng, *Met. Mater. Int.* **18**(1), 129 (2012)
- G.S. Fu, W.Z. Chen, K.W. Qian, *Chin. J. Nonferr. Met.* **12**, 269 (2002)
- G.M. Rusakov, A.G. Illarionov, Y.N. Loginov, M.L. Lobanov, A.A. Redikul'tsev, *Met. Sci. Heat Treat.* **56**(11–12), 650 (2015)
- G. Chen, G. Fu, S. Lin, C. Cheng, W. Yan, H. Chen, *Met. Sci. Heat Treat.* **54**(11–12), 623 (2013)
- Q.Y. Yang, Z.H. Deng, Z.Q. Zhang, Q. Liu, Z.H. Jia, G.J. Huang, *Mater. Sci. Eng. A* **662**, 204 (2016)
- C. Brozek, F. Sun, P. Vermaut, Y. Millet, A. Lenain, D. Embury, P.J. Jacques, F. Prima, *Scr. Mater.* **114**, 60 (2016)
- J.C. Tan, M.J. Tan, *Mater. Sci. Eng. A* **339**, 124 (2003)
- M.E. Kassner, M.M. Myshlyaev, H.J. McQueen, *Mater. Sci. Eng. A* **108**, 45 (1989)